Available online at www.sciencedirect.com
SCIENCE DIRECT®
Polymer 44 (2003) 8013–8023
polymer
www.elsevier.com/locate/polymer

Miscibility, thermal properties and polymorphism of syndiotactic polystyrene/poly(styrene-*co*-α-methyl styrene) blends

Fang-Chyou Chiu*, Ming-Te Li

Department of Chemical and Materials Engineering, Chang Gung University, Tao-Yuan 333, Taiwan, ROC

Received 30 May 2003; received in revised form 7 October 2003; accepted 15 October 2003

Abstract

This work examined the miscibility, crystallization kinetics, melting behavior and crystal structure of syndiotactic polystyrene (sPS)/poly(styrene-*co*-α-methyl styrene) blends. Differential scanning calorimetry, polarized light microscopy and wide angle X-ray diffraction technique were used to approach the goals. The single composition-dependent T_gs of the blends and the melting temperature (T_m) depression of sPS in the blends indicated the miscible characteristic of the blend system at all compositions. Furthermore, the T_gs of the blends could be predicted by either of the Gordon–Taylor equation (with $K = 0.99$) or the Fox equation with a slightly higher deviation. The dynamic and isothermal crystallization abilities of sPS were hindered with the incorporation of the miscible copolymer. Complex melting behavior was observed for melt-crystallized pure sPS and its blends as well. Nevertheless, the blends showed relatively simpler melting curves. Comparing with melt-crystallized samples, the cold-crystallized samples exhibited simpler melting behavior. The equilibrium melting temperature (T_m^0) of β form sPS crystal determined from the conventional extrapolative method is 295.2 °C. The Flory–Huggins interaction parameter, χ, of the blends was estimated to be -0.27. The crystal morphology of sPS was disturbed in the blends. Only underdeveloped granular-like crystalline superstructure of sPS exhibited in cold-crystallized blends. Moreover, the existence of the copolymer in the blends apparently reduced the possibility of forming the less stable α form sPS crystals.

Keywords: Syndiotactic polystyrene; Miscibility; Polymorphism

1. Introduction

Due to its performances, syndiotactic polystyrene (sPS) has been widely viewed as an emerging class of engineering thermoplastics [1]. Many investigations have characterized its complex polymorphic crystal structure [2–6]. Depending on the thermal treatments, four major crystalline forms (termed α, β, γ and δ) can be obtained. The α and β forms both possess a planar zigzag backbone conformation, and are confirmed as the predominant polymorphs encountered under normal crystallization conditions. Investigators have identified the α form as having a hexagonal [2,3] structure, whereas the β form packs in an orthorhombic [4] structure. The γ and δ forms consist of the similar monoclinic structure with both possessing a helical chain conformation [5,6]. Nevertheless, the γ and δ forms can only be obtained via solvent (e.g. dichloromethane and chloroform) induced crystallization.

The crystallization kinetics and melting behavior of sPS have also been investigated [7–17]. For instance, Cimmino et al. [7] noted that at the same undercoolings, the spherulite growth rate of sPS is more than one order of magnitude faster than that of isotactic polystyrene (iPS). The equilibrium melting temperature (T_m^0) (without mentioning which crystal form) was determined, using the extrapolative method, to be 275 °C. Hong et al. [12] observed that neat sPS shows three melting peaks after isothermal crystallizations. It was suggested that the lowest and the middle-melting peaks are attributed to the meltings of β and α form crystals, respectively; the highest-melting peak arises from the melting of recrystallized β form crystals. Woo and Sun et al. [13–15] further investigated the relationships between the polymorphic crystals and the resulting multiple melting peaks in sPS. For the bulk crystallization of sPS, Guerra et al. [16] reported that the polymorph (α or β or mixture forms) of the crystals formed depends strongly on factors such as its thermal history including the pre-melting

* Corresponding author. Tel.: +886-3-118800 X5297; fax: +886-3-2118668.
E-mail address: maxson@mail.cgu.edu.tw (F.C. Chiu).

0032-3861/$ - see front matter © 2003 Elsevier Ltd. All rights reserved.
doi:10.1016/j.polymer.2003.10.056

temperature, pre-melting time, as well the cooling rate and crystallization temperature.

Polymer blends with tailor-made properties continuously attract attention both academically and industrially [18]. Many of the commercial polymer blends are thus designed to satisfy synergistic improvements of their parent properties. However, the performances of blended products depend on the miscibility or 'compatibility' between the mixing components. To extend the versatility of sPS and overcome its brittleness, the sPS-based blends with requisite properties are expected to achieve. However, to our knowledge the sPS-based blends and compounds have been less investigated. So far the investigations have included sPS/atactic PS (aPS) system [19–22], sPS/poly(2,6-dimethylphenylene oxide) (PPO) system [12,13,23,24], and sPS/poly(vinyl methyl ether) (PVME) system [24,25]. The crystallization, melting behavior and crystal polymorph of sPS were found to be influenced by the incorporation of the guest polymers. For example, Wang et al. [20] found the simultaneous presence of positive and negative spherulites in the blends of sPS with aPS. Woo et al. [21] proved the miscibility of the sPS/aPS blends through various thermal transition approaches. The Flory–Huggins interaction parameter was thus determined. Guerra et al. [23] concluded that the addition of PPO but aPS would be favorable for the formation of the β polymorph in the sPS crystals. Cimmino et al. [24] reported that the spherulite growth rate of sPS decreases if PPO is added, whereas it increases with the addition of PVME. Nevertheless, the overall crystallization rate of sPS depresses with the addition of either PPO or PVME.

In our previous work [22], we have reported the effect of aPS molecular weight (MW) on the thermal properties and crystal polymorph of the sPS/aPS–50/50 blends. The smaller MW aPS was noted to influence the thermal properties and crystal polymorph of sPS the most. The profound dilution effect induced by the smaller MW aPS in the blends was taken into account for the observations. To date, the only miscible sPS-based blends that have been reported are sPS/PPO and sPS/aPS systems. From the practical and academic viewpoints, it will be inevitable to explore other sPS-based miscible blends. Therefore, in this study a potentially miscible counterpart for sPS, a styrene-based non-crystalline copolymer, is used to prepare the blend. The miscibility and thermal properties of the blend system are investigated. Special attentions are focused on the effect of incorporating the copolymer on the crystallization kinetics, melting behavior and the resulting polymorphism of sPS.

2. Experimental

2.1. Materials and blends preparation

Neat sPS resin manufactured by Idemitsu Kosan Co. Ltd, Japan was used in this study. Its number average MW, determined by GPC, is 2.20×10^5 g/mol. A non-crystalline poly(styrene-*co*-α-methyl styrene) copolymer purchased from Aldrich Chem. Co. was used to mix with sPS to prepare the blends with various compositions. The number average MW of the copolymer is determined by GPC to be around 5000 g/mol, which consisted of ca. 44 wt% of the styrene component. The blends were prepared using the solution mixing technique in order to avoid the possible thermal degradation of the samples at a high processing temperature. The mixing procedure involved dissolving weighted sPS and copolymer in 1,2,4-trichlorobenzene (TCB) to form solutions of 3 wt% at 130 °C. The solutions were then cast onto stainless dishes that were kept at 200 °C to rapidly evaporate the TCB solvent. To ensure complete solvent evaporation, the cast blends were exposed to a vacuum oven at 150 °C for at least 12 h before characterization. For comparative purposes, the parent sPS and copolymer were also TCB solvent treated.

2.2. Differential scanning calorimetry (DSC)

The thermal properties (including T_gs, crystallization kinetics and melting behavior) of the parent and blended samples were investigated using a Perkin Elmer DSC 7 analyzer equipped with an intra-cooler. The heat flow and temperature of differential scanning calorimetry (DSC) were calibrated with standard materials, such as indium and zinc. Nitrogen gas was consistently purged into the DSC during the scans to prevent specimens from thermal degradation at high temperatures. For T_g and cold crystallization investigations, the parent sPS and its blends were first melted at 310 °C for 2 min, and then quenched with liquid nitrogen to obtain amorphous characteristic. The amorphous specimens were further heated to determine the T_gs (at the 50% thermogram transitions) and the cold crystallization behavior. For melt crystallization experiments, the specimens were first melted at 310 °C, too. Upon the dynamic crystallization experiments, the specimens were cooled to room temperature at various rates. Upon the isothermal crystallization experiments, the specimens were quickly cooled to various pre-set temperatures (T_cs). The crystallized specimens were subsequently heated at 20 °C/min for the corresponding melting behavior investigations.

2.3. Polarized light microscopy (PLM)

Polarized light microscopy (PLM) was used to observe the crystal morphology of sPS with or without the copolymer incorporation. An Olympus BH-2 PLM with an attached CCD camera was employed in conjunction with a Linkam THMS 600 hot stage for these studies. The temperature of the hot stage was calibrated with benzoic acid (T_m = 122.5 °C). The thin-film pure sPS and blended specimens were prepared by casting the specimen-contained

TCB solution onto glass slides followed by keeping the specimens at 200 °C for 10 min under vacuum condition. Whereas the vacuum condition treatment ensured the complete solvent evaporation. The specimens were then thermally treated with different conditions, on the hot stage, for the crystal morphology observations.

2.4. Wide angle X-ray diffraction analysis (WAXD)

The wide angle X-ray diffraction (WAXD) spectra of crystallized specimens were recorded at room temperature using a Siemens D5005 X-ray unit. The X-ray used was Ni filtered Cu Kα radiation with a wavelength of 0.154 nm. The flat film technique was employed and the 2θ scan ranged from 2 to 40°. The content of the α form crystal in the specimens was quantitatively estimated via the following relation [16]:

$$P_\alpha(\%) = \frac{1.8A(11.6)/A(12.2)}{1 + 1.8A(11.6)/A(12.2)} \times 100\% \quad (1)$$

where 1.8 is the ratio between the intensities of the 2θ diffraction peak located at 11.6 and 12.2°, respectively, for specimens with the same thickness and crystallinity in the pure α and β forms. Meanwhile, $A(11.6)$ and $A(12.2)$ are the areas of the 2θ diffraction peaks located at 11.6 and 12.2°.

3. Results and discussion

3.1. Glass transition temperatures (T_gs)

The miscibility of binary blends is frequently ascertained by measurements of their T_gs. Fig. 1 shows the DSC heating thermograms of the amorphous samples in the glass transition temperature region. It is observed that the T_g of pure sPS and the copolymer is 99.1 and 70.1 °C, respectively. All the blends with different compositions exhibit single T_g which shifts to a higher temperature with the sPS content. This result suggests the miscibility of the two components in the blends when they are in the amorphous state. Further noted in the figure is the width of glass transition (ΔT_g) increases with increasing copolymer content. The ΔT_g ranges from ca. 11 °C of pure sPS to ca. 25 °C of pure copolymer. The determined T_gs along with the ΔT_gs of the samples are listed in Table 1. Due to the miscible character of the system, the comparisons among the T_gs of the experimental results and those predicted by the Gordon–Taylor equation [26] and the Fox equation [27] are made. These two equations are expressed as:

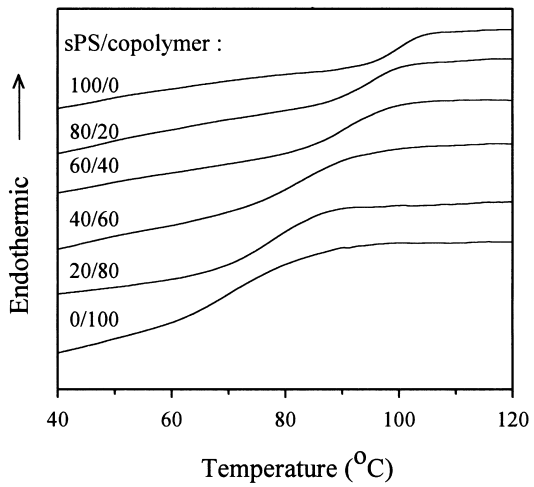

Fig. 1. DSC heating thermograms of the samples in the glass transition region.

Gordon–Taylor eq.:

$$T_g = T_{g1} + KW_2(T_{g2} - T_g)/W_1 \quad (2)$$

Fox eq.:

$$1/T_g = W_1/T_{g1} + W_2/T_{g2} \quad (3)$$

where 1 and 2 represent copolymer and sPS in our case, respectively; W_i is the weight fraction of component i. The K parameter is the ratio of the difference in thermal expansion coefficients between the rubbery and the glassy states for components 1 and 2. In fact, it is an adjusting parameter which has been served as a semi-quantitative measurement of the interaction strength between the mixed components [28,29]. Fig. 2 shows the Gordon–Taylor plot (T_g versus $W_2(T_{g2} - T_g)/W_1$) of the blends. A straight line is obtained through the least-squares method. According to Eq. (2), the slope of the straight line corresponds to the K parameter, and the intercept at $W_2(T_{g2} - T_g)/W_1 = 0$ represents the T_g of the copolymer. The K value estimated is 0.99, indicating the intimately mixed state of the two components. The fitted T_g (73.0 °C) of the copolymer is near the experimental data of 70.1 °C. Fig. 3 shows the experimental T_g data in comparison with the T_gs predicted by the Gordon–Taylor equation and the Fox equation. It is found that the experimental T_gs deviated slightly from the values predicted by both of the Gordon–Taylor (with

Table 1
Typical thermal data of the samples determined from DSC scans

Sample ID (sPS/copolymer)	100/0	80/20	60/40	40/60	20/80	0/100
T_g	99.1	93.6	90.1	82.6	77.3	70.1
ΔT_g	10.9	14.1	18.9	21.3	21.5	25.3
T_o [a]	250.2	243.5	233.5	229.6	NA	NA
T_{mc} [a]	244.3	234.2	222.2	215.7	NA	NA
T_o [b]	232.8	223.8	208.3	202.8	NA	NA
T_{mc} [b]	222.9	211.9	189.8	181.0	NA	NA
T_{mc} [a] − T_{mc} [b]	21.4	22.3	32.4	34.7	NA	NA
T_{cc} [c]	135.3	139.0	142.2	152.1	NA	NA
T_{cc} [d]	150.1	157.4	161.2	171.8	NA	NA
T_{cc} [d] − T_{cc} [c]	14.8	18.4	19.0	19.7	NA	NA

all units: °C. NA: not available.
[a] 2.5 °C/min cooled.
[b] 40 °C/min cooled.
[c] 10 °C/min heated.
[d] 40 °C/min heated.

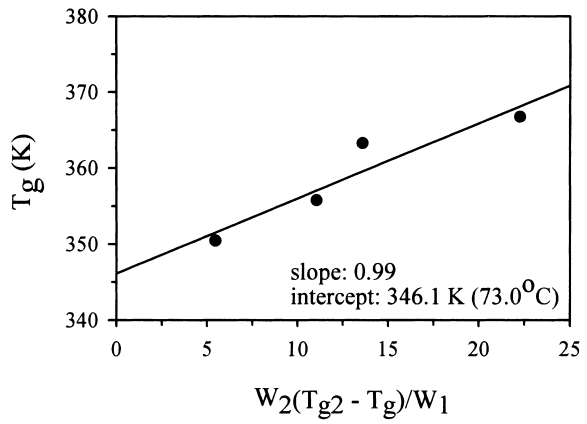

Fig. 2. Gordon–Taylor plot of the blends.

$K = 0.99$) and the Fox equations. This result suggests the components of the blends exhibit nearly ideal volume additivity. The even contributions of the two components' free volumes to the blends account for this observation. In addition to the single T_gs of the blends, the melting temperature (T_m) depression of sPS with the addition of the copolymer can also be taken as an evidence for the miscibility of the system (see below).

3.2. Crystallization behavior

Fig. 4 shows the DSC thermograms of pure sPS and its blends cooled from the melt at a rate of 2.5 and 40 °C/min, respectively. Regardless of the cooling rate, the addition of the non-crystalline copolymer depresses both of the sPS's crystallization onset temperature (T_o) and crystallization peak temperature (T_{mc}, temperature at the exotherm minimum). With increasing copolymer content, the T_o and T_{mc} further shift to lower temperatures and the crystallization peak width (ΔT_{mc}) broadens as well. These observations in fact imply the miscibility between the components in the molecular level. The 'poisoning' effect [30] incurred by the molecular

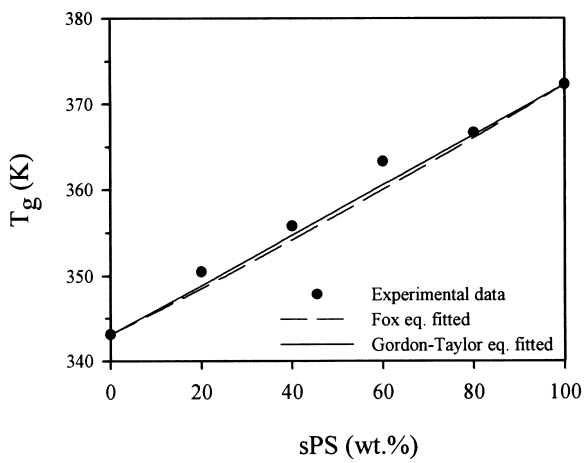

Fig. 3. Comparison of experimental determined T_gs with different equations fitted T_gs.

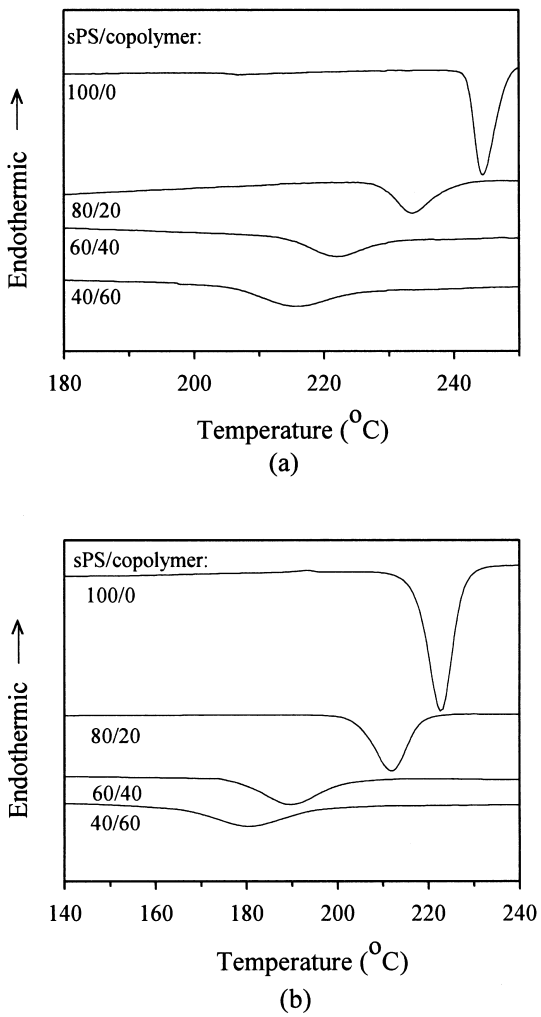

Fig. 4. DSC thermograms of sPS and its blends cooled from the melt with (a) 2.5 °C/min and (b) 40 °C/min.

segregation (rejection) of the non-crystalline copolymer from the nuclei or crystal growth front upon the sPS crystallization should play a dominant role in this issue. As well, if the blend possesses a higher copolymer content, a larger degree of copolymer segregation is needed for the initiation and completion of crystallization. Thus, the crystallization temperatures are depressed and the interval for crystallization is extended with the copolymer content. Comparing Fig. 4(a) with (b), it is also noted that a faster cooling rate shifts the T_o and T_{mc} of the samples to lower temperatures, and broadens the ΔT_{mc} as well. These phenomena are mostly ascribed to the fact that a slower cooling rate provides sufficient time for activating the sPS nuclei at higher temperatures. In contrast, the activation of sPS nuclei can only occur at lower temperatures at faster cooling rates [31]. Of course, the thermal lag effect is also accountable for the observations. But its effect should be minor due to the small sample size used in the experiments. Furthermore, it is noticed the T_{mc} depression with the cooling rate becomes larger as the copolymer content

increases in the samples. For example, the T_{mc} difference between 2.5 and 40 °C/min cooled samples is 21.4 °C for pure sPS, whereas the difference becomes 34.7 °C for the sample with 60% of the copolymer. This result is further indicative of the reduction of sPS's crystallization ability due to the occurrence of a higher level of copolymer segregation upon crystallization. The typical data obtained from DSC cooling scans are included in Table 1.

The cold crystallization behavior of sPS and its blends during the heating scans is also investigated. Fig. 5 depicts the typical results. Contrary to the behavior of composition-dependent T_{mc}, an increase in the copolymer content shifts the cold crystallization temperature (T_{cc}) of sPS to a higher temperature. This kind of retarded cold crystallization is not unusual for miscible blend systems. Two factors predominantly account for this kind of behavior. First is that the chain mobility of the crystallizable component is reduced due to a possibly higher T_g of the blend. Second is that the non-crystalline component causes a diluted environment (lower concentration) of the crystallizable component at the crystal growth front upon crystallization. Regarding our blend system, the T_g is ascertained to decrease with increasing non-crystalline copolymer content. Therefore, of the two factors the second factor should play a more dominant role in controlling the cold crystallization of our blends. The proximity of T_g values of the blends with various compositions causes the negligence of the first factor. The data obtained from the cold crystallization scans are included in Table 1.

The isothermal melt crystallization kinetics of the samples was studied at distinct T_cs via DSC. The crystallization peak time (t_p) is defined as the time when the exotherm minimum occurs. Fig. 6 shows the reciprocal value of t_p (i.e. t_p^{-1}) versus T_c for the selective crystallizable samples. Since t_p^{-1} is recognized to be proportional to the overall crystallization rate, the results clearly indicate that the copolymer inhibits the isothermal crystallization of sPS at an identical T_c. This feature corresponds well to the results of the dynamic melt crystallization study (Fig. 4). It is known, the isothermal crystallization rate of polymers basically depends on two energetic terms. One is the activation energy (ΔF^*) required for transporting the chain molecules across the melt-crystalline interface. The other is the free energy (ΔG^*), including enthalpic and entropic terms, required for the formation of a nucleus of critical size. The addition of a non-crystalline polymer to a crystallizable polymer may influence both the energetic terms, especially for a miscible blend. The influence on ΔF^* may be mainly accounted for by considering the variation of T_g with blend composition. That is at the same T_c, the sample with a lower T_g possesses a higher molecular mobility, and thus results in a lower ΔF^* value. Consequently, the crystallization rate of the lower T_g sample will be faster if the ΔG^* term effect of the samples is negligible. As a matter of fact, our results show that the samples with lower T_gs exhibit slower crystallization rates. This means the ΔF^* term exhibits a trivial effect on the isothermal melt crystallization of our samples at the T_c range investigated.

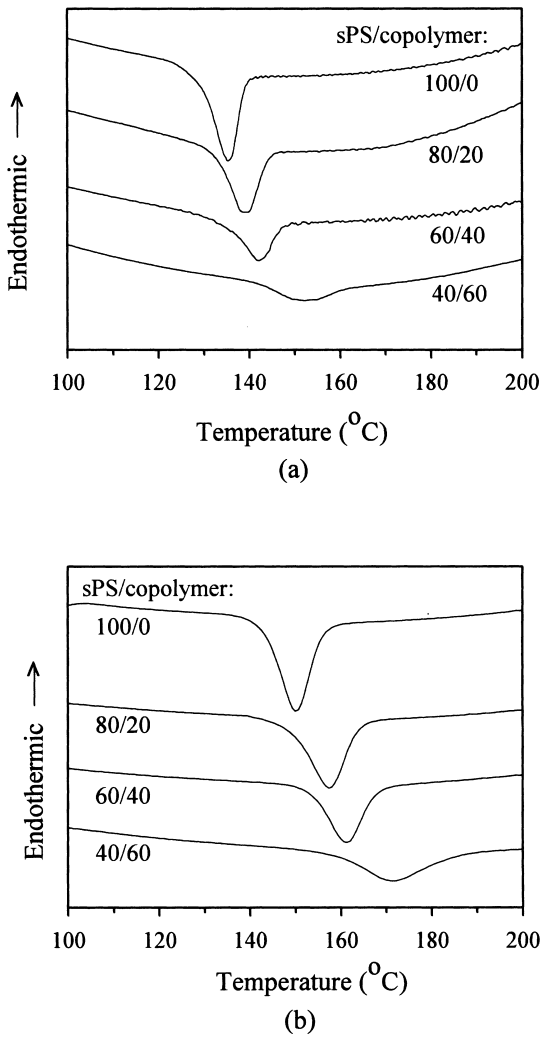

Fig. 5. DSC cold crystallization thermograms of the samples with a heating rate of (a) 10 °C/min and (b) 40 °C/min.

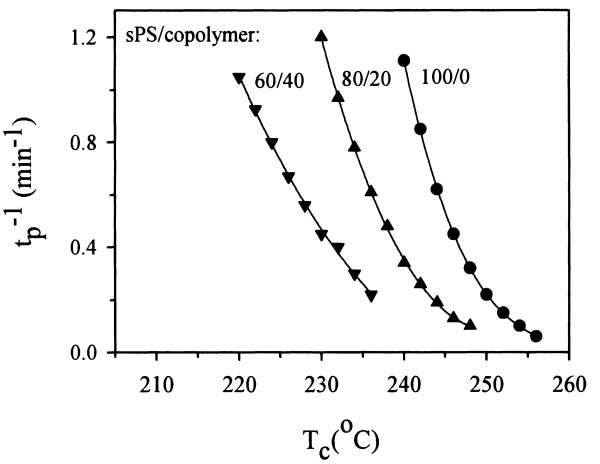

Fig. 6. Reciprocal crystallization peak time, t_p^{-1}, versus T_c for the selective samples.

Accordingly, the energetic ΔG^* term should play a dominant role in controlling the isothermal crystallization of our samples here. It is known if there are specific interactions between the components in the blends, a depression in the T_m^0 of the crystalline component occurs. As a result, the ΔG^* is higher for the sample with a lower T_m^0 while the samples are crystallized at the same T_c. Our results (see below) show that the addition of the copolymer indeed depresses the T_m^0 of sPS. The higher the copolymer content in the blend, the more the depression of the T_m^0 of sPS exhibits.

The well-known Avrami equation [32–34] is used to analyze the overall isothermal crystallization kinetics of the samples:

$$1 - X_t = \exp(-Kt^n) \tag{4}$$

which is always cast into

$$\ln[-\ln(1 - X_t)] = \ln K + n \ln t \tag{5}$$

where X_t is the fractional crystallinity at time t, n is the Avrami exponent and K is the kinetic parameter. As is widely recognized, the Avrami exponent can provide information on the nature of the nucleation and crystal growth geometry. The n determined from the Avrami plot (in the low crystallinity conversion region) is found to range from ca. 4 to ca. 6 as T_c increases for pure sPS. For the blends, the n value decreases. It ranges from ca. 2 to ca. 4 as T_c increases, and the value is further lowered for the blend having a higher copolymer content. According to Wunderlich [35], the n values of pure sPS suggest a thermal nucleation process followed by a three-dimensional crystal growth at lower T_cs. As T_c increases, the branching crystal growth evolves. The lower n values of the blends suggest the existence of copolymer changes the nucleation of sPS to athermal type, and/or the following crystal growth dimension is reduced. This result corresponds to the slower and incomplete crystallization of sPS as the copolymer content increases. The crystal morphology changes of sPS by the blending can be seen below.

3.3. Melting behavior

Fig. 7 shows the DSC melting curves of dynamically crystallized pure sPS and its blends. Note that, for both of the melt- and cold-crystallized samples, the T_m of sPS decreases as the copolymer content increases. This behavior indicates once again the miscible characteristic of the blends, though the crystals formed are not in a real state of equilibrium. In addition, simpler and smaller melting endotherms are observed for the cold-crystallized samples compared with those of melt-crystallized samples. This observation may imply the fact that the crystals formed through the melt crystallization process are more complex. As reported [9,14–16], polymorphism (α and β forms) and/or the occurrence of recrystallization–remelting process of β form crystals are frequently accounted for the complicated melting behavior of melt-crystallized sPS samples. On the other hand, for the cold-crystallized samples, α form crystals are predominantly observed in pure sPS, and β form crystals are dominated in the blends (see Section 3.5). No discernible recrystallization–remelting phenomenon of β form crystals is observed for the cold-crystallized samples.

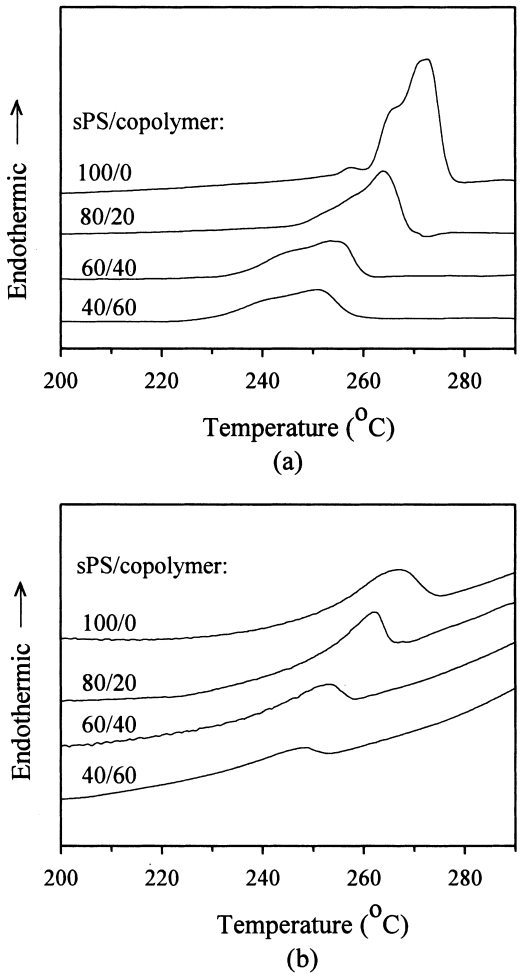

Fig. 7. DSC melting curves of the samples: (a) melt-crystallized with 40 °C/min and (b) cold-crystallized with 10 °C/min.

The representative DSC melting curves of isothermally crystallized (T_c = 240, 244 and 246 °C) pure sPS and its blend are shown in Fig. 8(a) and (b). Some features are worthy noting from these melting curves. First, the behavior of three distinct melting peaks become two apparent melting peaks (with an indistinct high-temperature shoulder) is observed for pure sPS as T_c increases; whereas only two melting peaks become one apparent melting peak is observed for the blend. One melting peak is evidently missing in the blend compared with pure sPS. Second, the lowest- and the middle-melting peaks of pure sPS as well as the low-melting peak of the blend shift to higher temperatures with T_c, but the high(est)-melting peaks of both samples stay nearly constant. Third, the intensity ratio between the low(est)-melting peak and the high(est)-melting peak increases with T_c for both samples. Regarding

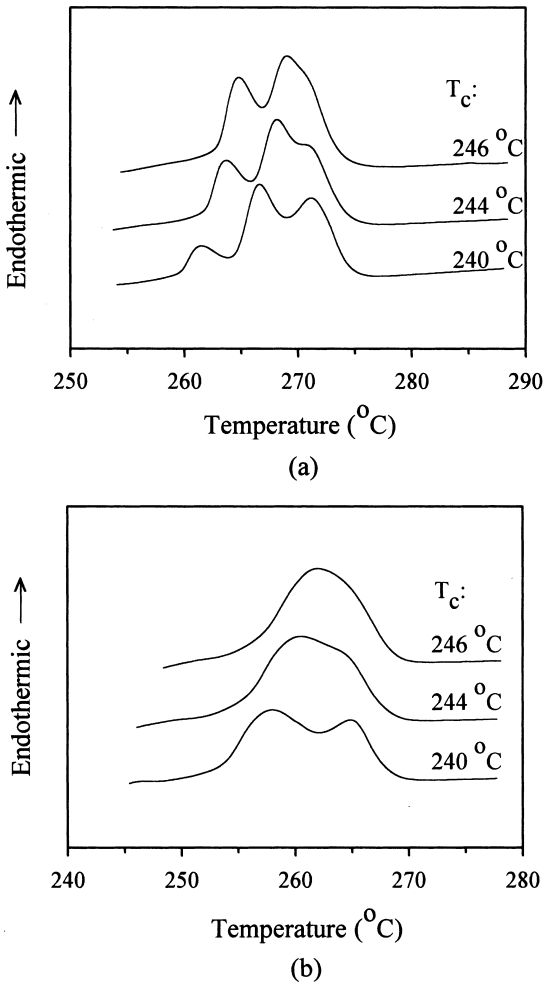

Fig. 8. Representative DSC melting curves of isothermally crystallized samples: (a) pure sPS and (b) sPS/copolymer–70/30.

the first feature, the WAXD structure analysis results indicate the missing melting peak in the blend corresponds to the middle-melting peak of pure sPS. It is associated with the absence or little amount of α form crystals in the blend. For the second and the third features, different heating-rate DSC experiments were conducted to reveal the origins. It is found a faster heating rate causes a higher intensity ratio between the low(est)-melting peak and the high(est)-melting peak. In addition, a faster heating rate seems to change the high(est)-melting peak position little, whereas the other melting peak(s) shift evidently to higher temperatures with the heating rate (not shown here for brevity). It is thus inferred the high(est)-melting peak associated crystals do not exist before the heating scans. The second and the third features resulted from the T_c effect on the degree of melting-recrystallization–remelting process of the β form crystals which are associated with the low(est)- and the high(est)-melting peaks. That is to say a higher T_c results in a more perfect β form crystal, and thus the possibility of recrystallization upon heating scans declines as well. Furthermore, comparing Fig. 8(a) with (b), the incorporation of copolymer causes a higher intensity ratio of the low(est)-melting peak to the high(est)-melting peak while the samples are crystallized at an identical T_c. This observation suggests the existence of the copolymer hinders the recrystallization ability of sPS.

The melting temperature, especially the T_m^0, is an important thermal property of a crystalline polymer or blend. For example, the degree of undercooling ($\Delta T = T_m^0 - T_c$) is a basic parameter for studying the kinetics of crystallization, and this value should be determined with the recognition of T_m^0 value. From the melting-curve figures depicted above, the T_m depression of sPS in the blends is evident. However, it is hardly possible to determine the T_ms of the thermodynamically stable β form sPS crystals at low T_cs because of the exhibition of complex melting peaks. Therefore, the original β form melting peaks (confirmed via WAXD) with low crystallinity for samples crystallized at high T_c region are used to estimate the β form T_m^0s through the conventional Hoffman–Weeks (HW) extrapolative method [36]. Fig. 9 depicts the HW T_m/T_c extrapolative plots of the samples. Using the least-squares fitting, each sample yields a straight line that intercepts with the $T_m = T_c$ line at a specific point, respectively. The determined T_m^0 value of pure β form sPS (295.2 °C) and those of its blends are included in Table 2. It is evident that the T_m^0 decreases as the copolymer content increases. However, it should be pointed out at this moment that the validity of using HW approach in determining the T_m^0 of a crystalline polymer has been reviewed by Marand et al. [37] recently. A so-called MX (non-linear HW) plot was thus proposed to correct the assumptions made in the original HW treatment. It was reported that the T_m^0 determined using the MX plot would be higher than that determined using the conventional HW plot. Nevertheless, more recently according to their experimental observations, Al-Hussein and Stroble [38] have commented on the inadequacy of using the MX plot. So, from our viewpoint, different arguments have their own limitations in determining the T_m^0. It is beyond the scope of the present study to conclude which method is the 'right'

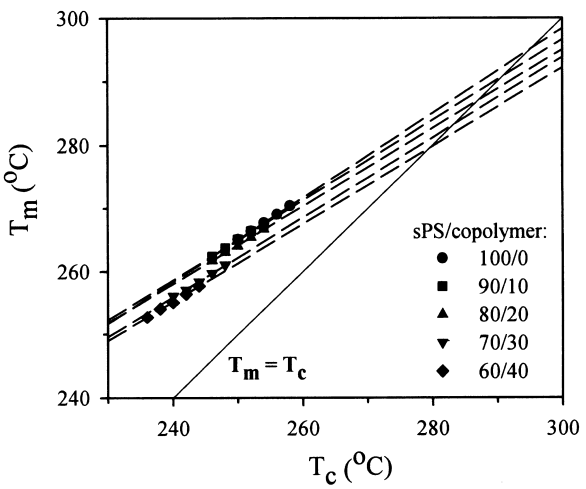

Fig. 9. Hoffman–Weeks plots of T_m against T_c for pure sPS and its blends.

Table 2
Equilibrium melting temperatures determined via HW extrapolative method

sPS/copolymer	100/0	90/10	80/20	70/30	60/40
T_m^0 (°C)	295.2	290.9	287.0	283.4	279.6

method in determining the T_m^0 value. As pointed out by Alamo et al. [39], if the experimental T_m is measured at very low levels of crystallinity (where the thickening effect of lamellae is greatly limited), the conventional HW plot is applicable in determining the T_m^0. Therefore, despite the arguments, the HW plot is still commonly used to date. Also, we want to mention that the T_m^0 value we determined for pure sPS is close to the value (292.7 ± 2.7 °C) determined based on the TEM results combined with the Gibbs–Thomson equation [40].

It is recognized the T_m^0 depression phenomenon in the blends can be used to evaluate the interaction parameter (χ) between the mixed components. The frequently used Flory–Huggins approximation [41] can be written as

$$\frac{1}{T_m^{0,b}} - \frac{1}{T_m^0} = -\frac{RV_2}{\Delta H_2 V_1}\left[\frac{\ln \Phi_2}{m_2} + \left(\frac{1}{m_2} - \frac{1}{m_1}\right) \times (1 - \Phi_2) + \chi(1 - \Phi_2)^2\right] \quad (6)$$

where subscript 1 and 2 denote the amorphous and crystallizable components, respectively; T_m^0 and $T_m^{0,b}$ are the equilibrium melting temperatures of the pure crystallizable component and its blends; χ is the interaction parameter; R is the gas constant; Φ_i, V_i and m_i are volume fraction, molar volume of repeating unit, and the degree of polymerization of component i. Owing to the relatively large values of m_1 and m_2 for polymer systems, Eq. (6) was exemplified by Nishi and Wang [42] as follows:

$$\frac{1}{T_m^{0,b}} - \frac{1}{T_m^0} = -\frac{RV_2}{\Delta H_2 V_1}\chi\Phi_1^2 \quad (7)$$

where it implies that a T_m^0 depression will yield a negative χ for the blends, indicating the miscible characteristic. While evaluating the χ parameter, the following values are used: $T_m^0 = 568.3$ K (295.2 °C); $V_2 = 92.9$ cm^3/mol (assuming the same as that of isotactic PS) [43]; $\Delta H_2 = 2050$ cal/mol [44]; $V_1 = 105$ cm^3/mol (estimating based on the relative ratio of styrene component and α-methyl styrene component in the sample) [45]. Fig. 10 shows a plot of $(1/T_m^{0,b} - 1/T_m^0)$ versus Φ_1^2. As it is shown, a linear line fitted with the least-squares method is obtained, and the χ value estimated from the slope is −0.27. Nevertheless, it is worthy mentioning that the result shown in Fig. 10 somewhat may be taken as a composition dependence of the

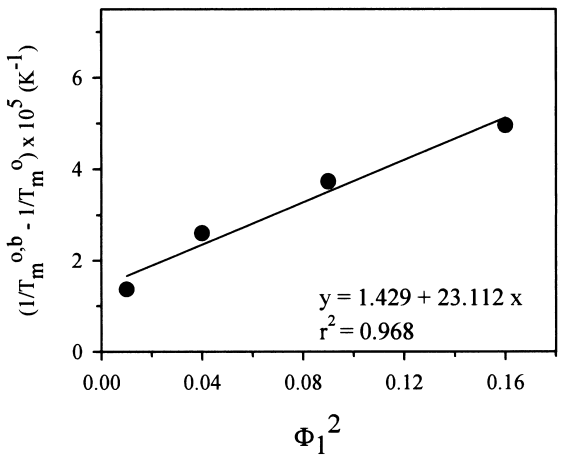

Fig. 10. Plot of $(1/T_m^{0,b} - 1/T_m^0)$ versus Φ_1^2 for selective blends.

interaction parameter. However, this suspicion cannot be rigorously concluded at this moment due to the slight scattering of the data points. Consequently, the χ value obtained can be deemed as an average value. Using the same approach, Woo et al. [21] have reported $\chi = -0.11$ for the miscible blends of sPS/aPS. It is believed that the lower χ value (−0.27) determined in our system is mainly attributed to the smaller MW of the non-crystalline copolymer component.

3.4. Crystal morphology

PLM is commonly used in the crystal morphology study of polymers. Fig. 11 depicts the representative PLM micrographs of samples melt-crystallized through two different conditions (i.e. air-quenched and 40 °C/min cooled). As shown in Fig. 11(a)–(c), the addition of copolymer evidently influences the crystal morphology of air-quenched sPS. The morphology of sPS transforms from a regular spherulite-like feature to a mostly underdeveloped rod-like feature. Also noted are the crystalline superstructure of sPS becomes smaller with increasing copolymer content, and more amorphous dark region exhibits as well. The evolution of crystal morphology confirms the reduction of the crystallization ability of sPS with the incorporation of the miscible counterpart. The influence of adding the copolymer on the crystal morphology of sPS is further shown in Fig. 11(d)–(g) of 40 °C/min cooled samples. The micrographs exhibit the gradually transformation of a regular spherulite-like superstructure to a disturbed (coarsened) superstructure of sPS. The boundaries between the superstructures are becoming diffuse as well. At other cooling rates, a similar kind of composition-dependent morphology can be observed. Moreover, while comparing the morphologies of the air-quenched samples with those of 40 °C/min cooled samples, it is noticed that a faster cooling rate results in a smaller crystalline superstructure of sPS. In addition, the crystal morphologies of dynamically cold-crystallized samples were also observed. In general, only

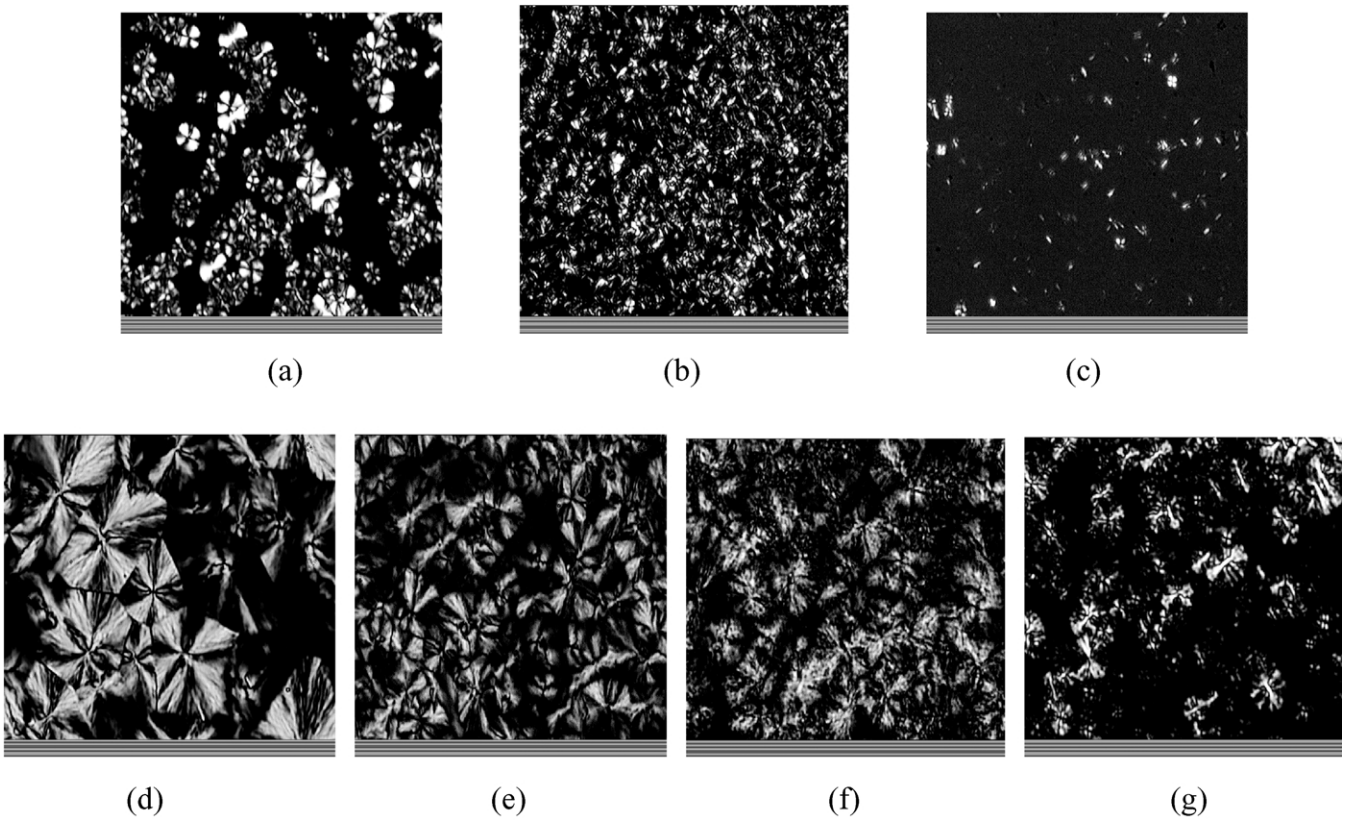

Fig. 11. PLM micrographs of melt-crystallized samples (sPS/copolymer): (a)100/0—air quenched; (b) 80/20—air quenched; (c) 60/40—air quenched; (d) 100/0—40 °C/min cooled; (e) 80/20—40 °C/min cooled; (f) 60/40—40 °C/min cooled and (g) 40/60—40 °C/min cooled.

tiny underdeveloped granular-like sPS superstructure is observed. The size of the granular superstructure becomes smaller as the copolymer content and the heating rate increase. The amount of the granular superstructure declines with the copolymer content.

3.5. Crystal structure

Fig. 12 shows the WAXD spectra of pure sPS and its blends crystallized from different conditions. As mentioned in Section 2, the intensities of the diffraction peaks located at $2\theta = 11.6$ and 12.2° are employed to estimate the content of the α form in the crystals. In Fig. 12(a) of melt-crystallized samples, both diffraction peaks with comparable intensity appear for pure sPS, indicating the crystals formed are mixtures of α form and β form. However, for the blends the intensity ratio between peaks located at $2\theta = 11.6$ and 12.2° decreases with increasing copolymer content. Only one diffraction peak ($2\theta = 12.2°$) is found for the blend with 80% of the copolymer. The percentage content of α form in the crystals formed under three different cooling conditions owing to Eq. (1) is listed in Table 3. It is concluded that the addition of the copolymer reduces the possibility of α form sPS crystal formation. The effect of the miscible counterpart on the polymorphism of its crystalline counterpart has been less reported. The observation in our system is suspected to be attributed to the T_m^0 depression of sPS in the blends, which results in a so-called higher 'pre-melting temperature' effect [10,16] on the resulting crystal structure of the samples. The phenomenon that a faster cooling rate causes a higher α form content is also noticed.

Fig. 12(b) shows the representative WAXD spectra of dynamically cold-crystallized samples. For pure sPS, a broader diffraction peak located around $2\theta = 11.6°$ is observed (without a noticeable $2\theta = 12.2°$ diffraction peak). This indicates that the sPS crystals thus formed mainly consisted of α form with certain size distribution. In contrast, the diffraction peak at $2\theta = 12.2°$ (with very minor or no diffraction peak at $2\theta = 11.6°$) exhibits evidently for the blends. For the samples that cold-crystallized with different rates, similar WAXD spectra are also observed. These results imply that, like that of melt-crystallized samples, the addition of the copolymer enhances the

Table 3
The percentage content of α form (P_α) crystals in melt-crystallized samples

	Sample ID (sPS/copolymer)				
Crystallization condition	100/0	80/20	60/40	40/60	20/80
2 °C/min cooled	53	36	13	<5	<5
10 °C/min cooled	64	41	21	<5	<5
40 °C/min cooled	78	66	39	12	<5

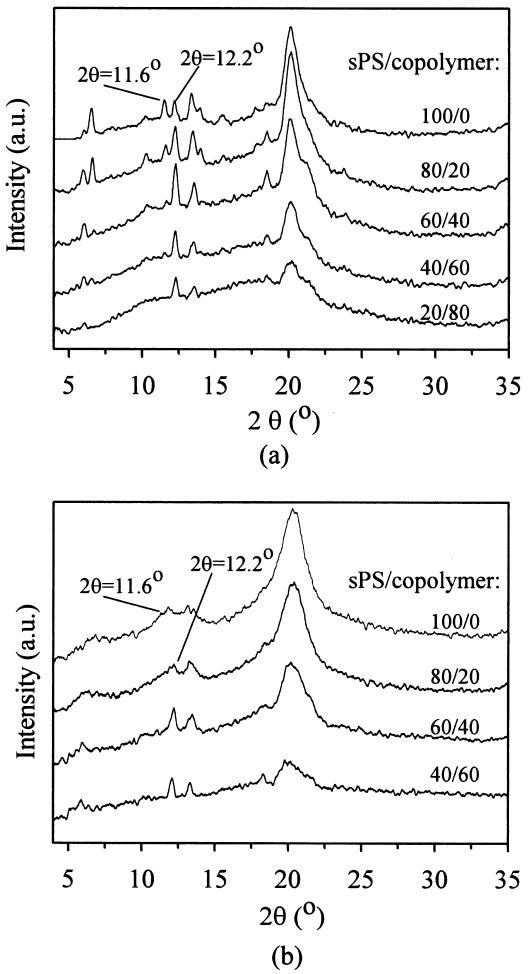

Fig. 12. WAXD spectra of sPS and its blends: (a) melt-crystallized with 10 °C/min and (b) cold-crystallized with 20 °C/min.

formation of the stable β form crystals in cold-crystallized samples under the crystallization conditions investigated. As we know, this kind of observation has never been reported before. The reason for this behavior is expected to be the same as that of the copolymer effect on the polymorphism of melt-crystallized samples. Nevertheless, to justify the explanation, supplementary experiments on the thermal history effect (e.g. pre-melting temperature, pre-melting time…) on the polymorphism of sPS and its blends are being conducted.

4. Conclusions

This study investigated the miscibility, thermal properties and crystal structure of sPS blended with poly(styrene-*co*-α-methyl styrene) copolymer. The single composition-dependent T_g*s* suggested that the blend system was miscible in the amorphous state. The Gordon–Taylor equation (with a *K* parameter of 0.99) and the Fox equation were appropriate in predicting the T_gs of the blends. The melt- and cold-crystallization abilities of sPS were both hampered with the addition of the miscible copolymer counterpart. The Avrami overall crystallization analysis revealed that the nucleation mechanism and crystal growth geometry of sPS were affected with the addition of the copolymer. The crystallization-condition-dependent multiple DSC melting peaks were observed for melt-crystallized pure sPS and its blends. However, the melting peaks were relatively simpler for the blends. The absence of the middle-melting peak of the blends was associated with the α form crystals. The dynamically cold-crystallized pure sPS and its blends all exhibited single but relatively broad melting peaks. Furthermore, the blends showed lower melting temperatures than that of pure sPS while the samples were crystallized through an identical condition. The T_m^0 of pure β form sPS was determined to be 295.2 °C, and the value decreases as the copolymer content increases. The Flory–Huggins interaction parameter (χ) thus estimated was −0.27. PLM experiments revealed that the crystal morphology of sPS was disturbed with the addition of the copolymer. The cold-crystallized blends exhibited an underdeveloped superstructure of sPS crystals. The WAXD results indicated the incorporation of the copolymer declined the α form crystal content regardless the samples were crystallized through melt crystallization or cold crystallization process. Furthermore, this effect was more evident as the copolymer content increased.

Acknowledgements

The authors would like to thank the National Science Council of the Republic of China for financially supporting this research. We also appreciate the valuable comments from Professor Stephen Z.D. Cheng of the University of Akron.

References

[1] Ishihara N, Seimiya T, Kuramoro M, Uoi M. Macromolecules 1986; 19:2464.
[2] Greis O, Xu Y, Asano T, Peterman J. Polymer 1989;30:590.
[3] Sun Z, Miller RL. Polymer 1993;34:1963.
[4] De Rosa C, Rapacciuolo G, Guerra G, Petraccone V, Corradini P. Polymer 1992;33:1423.
[5] Chanati Y, Shimane Y, Inagaki T, Ijitsu T, Yukinari T, Shikuma H. Polymer 1993;34:1620.
[6] Chanati Y, Shimane Y, Inoue Y, Inagaki T, Ishioka T, Ijitsu T, Yukinari T. Polymer 1992;33:488.
[7] Cimmino S, Di Pace E, Martuscelli E, Silvestre C. Polymer 1991;32: 1080.
[8] Wesson RD. Polym Engng Sci 1994;34:1157.
[9] Chiu FC, Peng CG, Fu Q. Polym Engng Sci 2000;40:2397.
[10] Chiu FC, Shen KY, Tsai SHY, Chen CM. Polym Engng Sci 2001;41: 881.
[11] Wu HD, Wu ID, Chang FC. Macromolecules 2000;33:8915.
[12] Hong BK, Jo WH, Lee SC, Kim J. Polymer 1998;39:1793.
[13] Woo EM, Wu FS. Macromol Chem Phys 1998;199:2041.

[14] Sun YS, Woo EM. Macromolecules 1999;32:7836.
[15] Woo EM, Sun YS, Yang CP. Prog Polym Sci 2001;26:945.
[16] Guerra G, Vitagliano VM, De Rosa C, Petraccone V, Corradini P. Macromolecules 1990;23:1539.
[17] Li Y, He J, Qiang W, Hu X. Polymer 2002;43:2489.
[18] Utracki LA. Commercial polymer blends. New York: Chapman & Hall; 1998.
[19] Hong BK, Jo WH, Kim J. Polymer 1998;39:3753.
[20] Wang C, Chen CC, Cheng YW, Liao WP, Wang ML. Polymer 2002; 43:5271.
[21] Woo EM, Lee ML, Sun YS. Polymer 2000;41:883.
[22] Chiu FC, Peng CG. Polymer 2002;43:4879.
[23] Guerra G, De Rosa C, Vitagliano VM, Petraccone V, Corradini P. J Polym Sci, Polym Phys 1991;29:265.
[24] Cimmino S, Di Pace E, Martuscelli E, Silvestre C. Polymer 1993;34: 2799.
[25] Cimmino S, Di Pace E, Martuscelli E, Silvestre C, Rice DM, Karasz FE. Polymer 1993;34:214.
[26] Gordon M, Taylor JS. J Appl Chem 1952;2:493.
[27] Fox TG. Bull Am Phys Soc 1956;1:123.
[28] Belorgey G, Aubin M, Prud'homme RE. Polymer 1982;23:1051.
[29] Chiu FC, Min K. Polym Int 2000;49:223.
[30] Cheng SZD, Lots B. Philos Trans R Soc London, Ser A 2003;361:517.
[31] Lopez LC, Wilkes GL. Polymer 1989;30:882.
[32] Avrami M. J Chem Phys 1939;7:1103.
[33] Avrami M. J Chem Phys 1940;8:212.
[34] Avrami M. J Chem Phys 1941;9:177.
[35] Wunderlich B, Macromolecular physics, vol. 2. New York: Academic Press; 1976.
[36] Hoffman JD, Weeks JJ. J Res NBS, A Phys Chem A 1962;66:13.
[37] Marand H, Xu J, Srinivas S. Macromolecules 1998;31:8219.
[38] Al-Hussein M, Strobl G. Macromolecules 2002;35:1672.
[39] Alamo RG, Chan EKM, Mandelkern L, Voigt-Martin IG. Macromolecules 1992;25:6381.
[40] Wang C, Cheng YW, Hsu YC, Lin TL. J Polym Sci, Polym Phys 2002;40:1626.
[41] Flory PJ. Principles of polymer chemistry. New York: Cornell University Press; 1953.
[42] Nishi T, Wang TT. Macromolecules 1975;8:909.
[43] Runt JP. Macromolecules 1981;14:420.
[44] Gianotti G, Valvassori A. Polymer 1990;31:473.
[45] Van Krevelen DW. Properties of polymers, their estimation and correlation with chemical structure. Amsterdam: Elsevier; 1976.